Nonlinear Interaction Between Signal and Noise in Optical Fibers

Armando N. Pinto, *Senior Member, IEEE, Member, OSA*, and Govind P. Agrawal, *Fellow, IEEE, Fellow, OSA*

***Abstract*—A model suitable for analyzing the nonlinear interaction between signal and noise, mediated by the Kerr effect in optical communication systems, is presented. This model treats separately signal and noise and permits analysis of the symbols' central time position and frequency evolution. It is shown that this nonlinear interaction between signal and noise leads to symbols' random frequency shifts, which induce timing jitter in all types of systems. We also discuss the problem of estimating timing jitter for a signal embedded in noise.**

***Index Terms*—Optical fiber communication, optical Kerr effect, optical noise, timing jitter.**

I. Introduction

SIGNAL and noise interact in optical fibers through the Kerr effect, which is responsible for the intensity dependence of the modal refractive index. This interaction has mostly been studied in the context of soliton communication systems [1]–[3]. Based on the particle-like nature of solitons, a perturbation theory was developed [4] that allows the treatment of the signal separately from the noise, considering the effect of the nonlinear interaction between signal and noise. This soliton and noise interaction mediated by the Kerr effect is generally referred as the Gordon–Haus effect [2] and leads to a type of timing jitter that grows cubically with the distance. Timing jitter growing cubically with the distance was also found in linear communication systems [5], even though the origin of this jitter is not the Gordon–Haus effect, because signal and noise do not interact along the transmission channel in the absence of nonlinear effects.

A linear model is not able to describe accurately modern high-bit-rate optical communication systems, and these systems are not necessarily soliton communication systems. Consequently, the perturbation theory developed for solitons cannot also be applied. Therefore, the study of the nonlinear interaction between signal and noise in nonsoliton systems is an open issue. Such a study has not advanced further due to the lack of an accurate mathematical model that allows one to separate the signal from the noise but still accounts for the nonlinear interaction between the two, as perturbation theory does for the particular case of soliton communications systems. In [6], we addressed this problem considering that the noise propagates over a linear channel. However, a more accurate model can be obtained if the effects of the signal on the noise, mediated by the Kerr effect, are considered.

In this paper, we present a model that is able to treat separately the signal and noise but still accounts for the nonlinear interaction between the two. Using this model, we prove that indeed the signal and noise interaction, mediated by the Kerr effect in optical fibers, causes random shifts in the symbols' central frequency in virtually all types of systems, and these shifts lead to timing jitter. This is not a particular characteristic of soliton communication systems, and only idealized linear transmission systems do not suffer from this effect.

This paper is organized as follows. In Section II, we present the new mathematical model proposed to study the interaction between signal and noise in optical communication systems. Results related with the extensive validation of the model are presented in Section III. We analyze, in Section IV, the symbols' random frequency shifts. The several contributions to timing jitter are numerically estimated in Section V. Comparisons are made between the solutions obtained using the proposed model and the results obtained with the standard model based on the resolution of the nonlinear Schödinger (NLS) equation. The main conclusions of this paper are presented in Section VI.

II. Mathematical Model

The propagation of an electromagnetic field through an optical fiber can be modeled using the NLS equation [7]

$$\frac{\partial A}{\partial z} + i\frac{\beta_2}{2}\frac{\partial^2 A}{\partial t^2} + \frac{\alpha}{2}A = i\gamma|A|^2 A \tag{1}$$

where $A(z,t)$ is the complex amplitude of the electric field, normalized such that $|A(z,t)|^2$ equals the optical power. The independent variables z and t represent, respectively, the propagation distance, measured from the beginning of the system, and the time measured in a reference frame that moves at the speed

$$v_g(\omega_s(0)) = \frac{1}{\beta_1(0)} \tag{2}$$

with

$$\beta_1(0) = \frac{\partial \beta(\omega)}{\partial \omega} \tag{3}$$

Manuscript received July 10, 2007; revised September 7, 2007. Published August 29, 2008 (projected). This work was supported in part by the Portuguese scientific foundation (FCT) under a Sabbatical Grant in the context of the "QUANTUM" project and in part by the European Union under the FEDER program.

A. N. Pinto is with the Department of Electronics, Telecommunications and Informatics, University of Aveiro, and the Institute of Telecommunications, 3810-193 Aveiro, Portugal (e-mail: anp@ua.pt).

G. P. Agrawal is with the Institute of Optics, University of Rochester, Rochester, NY 14627 USA (e-mail: gpa@optics.rochester.edu).

Digital Object Identifier 10.1109/JLT.2007.912029

where the first derivative of the propagation constant $\beta(\omega)$ is evaluated at a given frequency $\omega_s(0)$, which we choose to coincide with the signal's central frequency at the system input $z = 0$. The parameter β_2 is the second derivative of $\beta(\omega)$ evaluated at $\omega_s(0)$ and accounts for the group velocity dispersion, α accounts for the optical attenuation, and γ accounts for the Kerr effect.

In order to compensate for optical losses, modern lightwave telecommunications systems use optical amplification. Optical amplifiers restore the power of the signal but also add noise that copropagates with the signal. The effect of amplifiers can be considered by using the following boundary condition in the resolution of (1):

$$A(z = nL_a^+, t) = \sqrt{G_n}A(z = nL_a^-, t) + N_n(0, t) \tag{4}$$

where $z = nL_a^-$ and $z = nL_a^+$ are the locations immediately before and after the nth amplifier and G_n and $N_n(0, t)$ are the nth amplifier gain and the complex amplitude of the amplified spontaneous emission noise added by the nth amplifier, respectively. Consequently, at any point of an optical communication system, the electric field can be written as the sum of a signal $S(z, t)$ that conveys the information and noise $N(z, t)$ that limits our ability to extract information from the signal. Therefore, without loss of generality, we can write

$$A(z, t) = S(z, t) + N(z, t) \tag{5}$$

with $A(z, t)$ satisfying (1). The signal $S(z, t)$ is a collection of symbols, each transporting a given amount of information, typically, a single bit.

Equation (1) has been used to assess the performance of optical telecommunication systems, but its use to study the interaction between signal and noise in the transmission channel is limited. For instance, it is not possible to obtain from (1) either the evolution of the symbols' central position or the evolution of the symbols' central frequency.

We can define the central position of the field intensity profile within a given time window T_w in the usual way as

$$t_t(z) = \frac{1}{E_s(z)} \int_{-T_w/2}^{+T_w/2} t|A(z, t)|^2 dt \tag{6}$$

where

$$E_s(z) = \int_{-T_w/2}^{+T_w/2} |S(z, t)|^2 dt \tag{7}$$

with T_w chosen in such a way that

$$E_s(z) \approx \int_{-\infty}^{+\infty} |S(z, t)|^2 dt. \tag{8}$$

However, it is important to stress that $t_t(z)$ should not be confused with the symbol's central position, even in the case where there is a single symbol in the time window T_w, which is the case that we always assume in this paper. Indeed, by substituting (5) in (6), we can see that

$$t_t(z) = t_s(z) + t_n(z) + t_{sn}(z) \tag{9}$$

where

$$t_s(z) = \frac{1}{E_s(z)} \int_{-T_w/2}^{+T_w/2} t|S(z, t)|^2 dt \tag{10}$$

$$t_n(z) = \frac{1}{E_s(z)} \int_{-T_w/2}^{+T_w/2} t|N(z, t)|^2 dt \tag{11}$$

and

$$t_{sn}(z) = \frac{1}{E_s(z)} \int_{-T_w/2}^{+T_w/2} tS(z, t)N^*(z, t)dt + \frac{1}{E_s(z)} \int_{-T_w/2}^{+T_w/2} tN(z, t)S^*(z, t)dt \tag{12}$$

with $N(z, t)$ assumed to be bandlimited in the spectral domain in order to guarantee that the integral in (11) converges. From (9), we see that $t_t(z)$ is the sum of three terms: the first one is the symbols' central position $t_s(z)$, the second one is the noise's central position $t_n(z)$ within the time window T_w, and the third one has its origin in the signal-to-noise beating $t_{sn}(z)$. Using (1), we can estimate $t_t(z)$ but cannot determine $t_s(z)$ because we do not know $t_n(z)$ nor $t_{sn}(z)$. An analogous situation happens for the symbols' central frequency. We can define

$$\omega_t(z) = \frac{1}{E_s(z)} \int_{-\Omega_w/2}^{+\Omega_w/2} \omega|\tilde{A}(z, \omega)|^2 d\omega \tag{13}$$

but, again, $\omega_t(z)$ should not be confused with the symbol's central frequency. Indeed, $\omega_t(z)$ is given by

$$\omega_t(z) = \omega_s(z) + \omega_n(z) + \omega_{sn}(z) \tag{14}$$

where

$$\omega_s(z) = \frac{1}{E_s(z)} \int_{-\Omega_w/2}^{+\Omega_w/2} \omega|\tilde{S}(z, \omega)|^2 d\omega \tag{15}$$

$$\omega_n(z) = \frac{1}{E_s(z)} \int_{-\Omega_w/2}^{+\Omega_w/2} \omega|\tilde{N}(z, \omega)|^2 d\omega \tag{16}$$

and

$$\omega_{sn}(z) = \frac{1}{E_s(z)} \int_{-\Omega_w/2}^{+\Omega_w/2} \omega\tilde{S}(z, \omega)\tilde{N}^*(z, \omega)d\omega + \frac{1}{E_s(z)} \int_{-\Omega_w/2}^{+\Omega_w/2} \omega\tilde{N}(z, \omega)\tilde{S}^*(z, \omega)d\omega \tag{17}$$

with Ω_w being the noise spectral bandwidth, assumed to be much broader than the signal spectrum. $\tilde{A}(z, \omega)$, $\tilde{S}(z, \omega)$, and

$\tilde{N}(z,\omega)$ represent the Fourier transforms of the field, signal, and noise, respectively. The three terms in (14) are the symbol's central frequency, $\omega_s(z)$, the noise's central frequency, $\omega_n(z)$, and $\omega_{sn}(z)$, which has its origin in the signal-to-noise beating. They can be evaluated using (15)–(17), respectively, as long as the signal and noise spectrum evolution along the transmission channel are known. Unfortunately, this cannot be obtained from (1) due to the nonlinear nature of the NLS equation.

In summary, (1) does not provide a separate description of the signal and noise evolution along the transmission channel. It only describes the evolution of the entire field. A major purpose of this paper is to present a new model that describes separately the signal and noise evolution along the transmission channel but still considers the nonlinear interaction between the two. To achieve that, we start by replacing (5) in (1). After that, the right-hand side of (1) consists of six terms. By using physical reasoning, we found that (1) can indeed be split in two equations: one equation for the signal, which includes two of these six terms, and another for the noise, which includes the other four terms, i.e.,

$$\frac{\partial S}{\partial z} + i\frac{\beta_2}{2}\frac{\partial^2 S}{\partial t^2} + \frac{\alpha}{2}S = i\gamma|S|^2 S + i\,2\gamma|N|^2 S \tag{18}$$

and

$$\frac{\partial N}{\partial z} + i\frac{\beta_2}{2}\frac{\partial^2 N}{\partial t^2} + \frac{\alpha}{2}N = i\gamma|N|^2 N + i\,2\gamma|S|^2 N + i\gamma S N^* S + i\gamma N S^* N. \tag{19}$$

To see that (18) and (19) make sense from a physical point of view, consider first the linear case. If we place γ equal to zero in both equations, we obtain two independent equations: one for the signal and another for the noise. This is the expected result, as signal and noise propagate independently in a linear channel. In fact, our model can be derived exactly from (1), without any approximation or assumption for the linear case. Consider now the nonlinear case $\gamma \neq 0$: if either the signal or the noise is absent, we end up with (1) in both cases, as expected. When both signal and noise are present, the only extra term that appears in the signal equation is that related to the cross-phase modulation produced on the signal by the noise. An equivalent term appears in the noise equation, so if we neglect the last two terms in the noise equation, these equations are identical. The only difference arises from the four-wave-mixing terms, which enhance the noise by transferring energy between the signal and the noise. In the first four-wave mixing term of (19), the signal acts as a pump and noise is amplified. In the second term, noise acts as a pump and the signal is amplified. But because noise fluctuates, extra noise is added to the signal in both cases. Thus, the four-wave mixing terms always give rise to excess noise. This is the reason why both four-wave mixing terms appear in the noise equation and not in the signal equation.

III. Validation of the Model

From the discussion in the previous section, we see that $t_s(z)$ can be calculated from (9) if (1) is used to obtain $t_t(z)$ and (18) and (19) are used to calculate $t_n(z)$ and $t_{sn}(z)$, respectively. However, if (18) and (19) describe accurately the signal and noise evolution, it should also be possible to obtain $t_s(z)$ from the symbol's group velocity $v_g(\omega_s(z))$ evolution along the transmission channel

$$t_s(z) = \int_0^z \frac{d\zeta}{v_g(\omega_s(\zeta))} - \frac{z}{v_g(\omega_s(0))}. \tag{20}$$

Because $1/v_g = \beta_1$, we can write

$$t_s(z) = \int_0^z \beta_1(\omega_s(\zeta))d\zeta - \beta_1(\omega_s(0))\,z \tag{21}$$

and by considering

$$\beta_1(\omega_s(\zeta)) \simeq \beta_1(\omega_s(0)) + \beta_2(\zeta)\,[\omega_s(\zeta) - \omega_s(0)] \tag{22}$$

we obtain

$$t_s(z) = \int_0^z \beta_2(\zeta)\,[\omega_s(\zeta) - \omega_s(0)]\,d\zeta. \tag{23}$$

The ζ dependence of β_2 in (22) and (23) allow for the possibility of using fibers with different group velocity dispersion values along the transmission channel, for instance, to achieve dispersion compensation. Note that $\omega_s(\zeta)$ in (23) can be evaluated using (15) together with (18) and (19).

From (23), it is also clear that $t_s(z)$ tends to be small if the average value of the group velocity dispersion approaches zero. This leads to systems with low timing jitter, as was shown experimentally, for example, in [8].

In order to validate our model, we compare the values of $t_s(z)$ obtained using (9) with those obtained using (23), for different propagation regimes.

Previously, we have shown that our model is exact for the linear case. Now we investigate how well it performs in a highly nonlinear case. We consider a 10-Gb/s average soliton communication system. The signal after the booster amplifier is given by $S(z,0) = \sqrt{(P_0)}\mathrm{sech}\,(t/T_0)$, with P_0 and T_0 the soliton peak power and pulse width, respectively. We assume that the system operates over fibers with losses of 0.2 dB/km, group velocity dispersion of -2 ps^2/km, and a nonlinear coefficient of 1.3 W^{-1}/km. The soliton temporal width T_0 was adjusted to be 1/5 of the bit period, i.e., 20 ps, which leads to a dispersion length $L_D = T_0^2/|\beta_2|$ of 200 km. The soliton peak power P_0 is approximately 18 mW, and the signal is amplified every 100 km. The gain of the amplifiers equals 20 dB with a noise spontaneous emission factor [7], n_{sp}, of 1.0. The soliton and noise copropagate during ten dispersion lengths (2000 km).

Fig. 1(a) shows the evolution of the soliton center position along the transmission line for five different realizations of the noise. Solid lines are obtained from $t_s(z) = t_t(z) - t_n(z) - t_{sn}(z)$ [see (9)], with $t_t(z)$ being evaluated using the NLS equation [see (1)] and $t_n(z)$ and $t_{sn}(z)$ calculated using (11) and (12), respectively. Filled circles are obtained using (23), with $\omega_s(z)$ obtained from (15). $S(z,t)$ and $N(z,t)$ are calculated from (18) and (19), respectively. We can see a good agreement

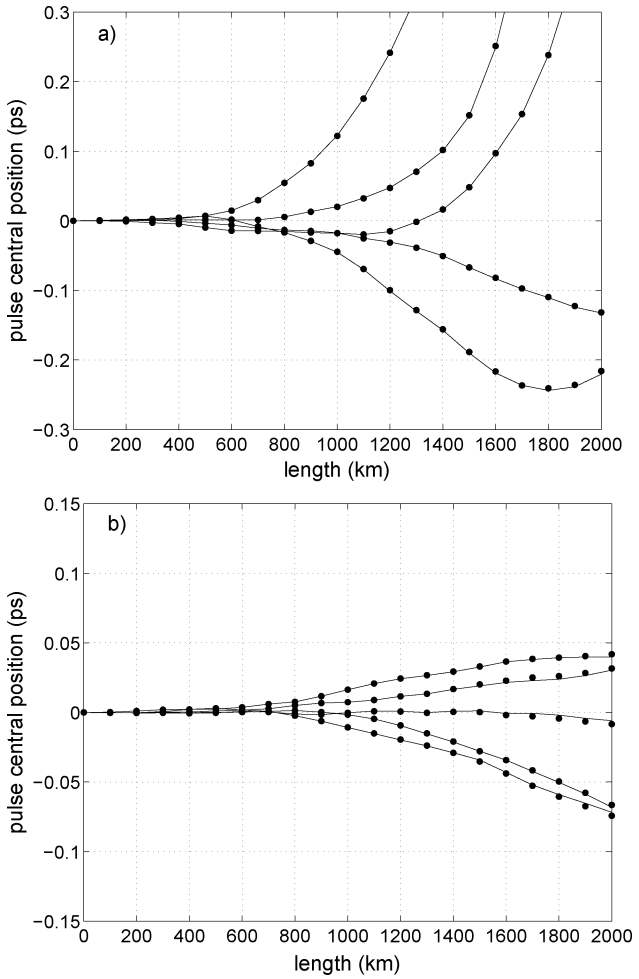

Fig. 1. Pulse central position evolution for (a) soliton and (b) nonsoliton communication system. In each case five different noise realizations are considered. Solid lines are obtained using (9) together with (1), (11), and (12). Filled circles are obtained from (23) jointly with (15), (18), and (19).

for the soliton's central position evolution, which proves that our model describes accurately the soliton's central position and frequency evolution.

In Fig. 1(b), a nonsoliton system is considered. We consider a Gaussian-shape pulse, with 20 ps of root-mean-square (rms) pulse temporal width and a peak power of 5 mW after the booster amplifier. In order to manage the chromatic dispersion, each span is composed of 80 km of standard single-mode fiber, with group velocity dispersion of -2 ps^2/km and a dispersion compensation fiber of 20 km, with group velocity dispersion of 8 ps^2/km. We assume that both fibers have losses of 0.2 dB/km and a nonlinear coefficient of 1.3 W^{-1}/km. The amplifiers have 20 dB of gain and n_{sp} of 1.0. Again, we can see a good agreement between the values for the pulses' central position evolution calculated using (9) and those obtained from (23).

We perform a similar test for several systems with different degrees of nonlinearities and with different dispersion management techniques. For all the considered systems, a very accurate description of the pulses' central position evolution is verified. These results clearly show that the new proposed model describes accurately the signal and noise evolution in a separate way, even for highly nonlinear systems, as in the case of soliton communication systems.

IV. Random Frequency Shifts

In the preceding section, we showed how the symbols' central position evolves along the transmission channel. We also pointed out that this temporal evolution is directly related with the evolution of the symbols' central frequency. In this section, we analyze how the symbols' central frequency evolves.

It is worth noting that in direct detection receivers, phase is lost during the detection process. For this type of receiver the symbols' temporal position tends to be the critical aspect, as its random fluctuations lead to suboptimum operation of the decision circuit. However, if homodyne or heterodyne detection is employed, the stability of the symbols' central frequency becomes a relevant issue, as large fluctuations can lead to strong deterioration of the receiver performance. Modern semiconductor lasers have spectral linewidths of less than 10 MHz. However, frequency fluctuations due to signal and noise nonlinear interaction in optical fibers can easily become larger than that. Therefore, this aspect must be considered in the design of homodyne and heterodyne receivers. Large fluctuations in the symbols' central frequency also preclude the use of narrow optical filters and lead to a less efficient use of the optical spectrum.

Fig. 2(a) and (b) shows the evolution of the pulses' central frequency along the transmission channel for a soliton and a nonsoliton communication system. The (a) soliton and (b) nonsoliton communication systems considered are the same described in detail in the preceding section.

There are several features worth noting in the results presented in Fig. 2. First, comparing the results presented in Fig. 1 with those presented in Fig. 2, we can observe that the curves for the evolution of symbols' central position are smoother than those for the symbols' central frequency evolution. This happens because the symbol's central position and frequency are related by the integral presented in (23). Other aspect is that shifts in the central frequency tend to occur immediately after an amplifier. Note that amplifiers are placed 100 km apart. That should be no surprise, as these shifts have their origin in the nonlinear interaction between signal and noise, and thus they tend to occur where the nonlinear effects are stronger, i.e., right after the amplifiers where signal and noise powers are highest. However, frequency shifts do not occur instantaneously after amplifiers but occur progressively as the signal propagates. This is an important point because, in the context of soliton theory, it is frequently assumed that shifts occur instantaneously, but this is in fact an approximation, as our results show. Indeed, for a pure soliton, i.e., assuming a lossless soliton system, shifts occur throughout the transmission channel because nonlinear effects remain strong over the whole system length. Another interesting aspect is related to the direction of the shifts. It is quite clear from Fig. 2 that the direction of the shifts remains strongly correlated with the direction of the first shift for quite a long distance. That feature is also observable in Fig. 1, as we see that in most cases the symbols' center position evolves without changing direction. It means that the effect of the noise added by the first amplifier plays a dominant role. This effect eventually vanishes

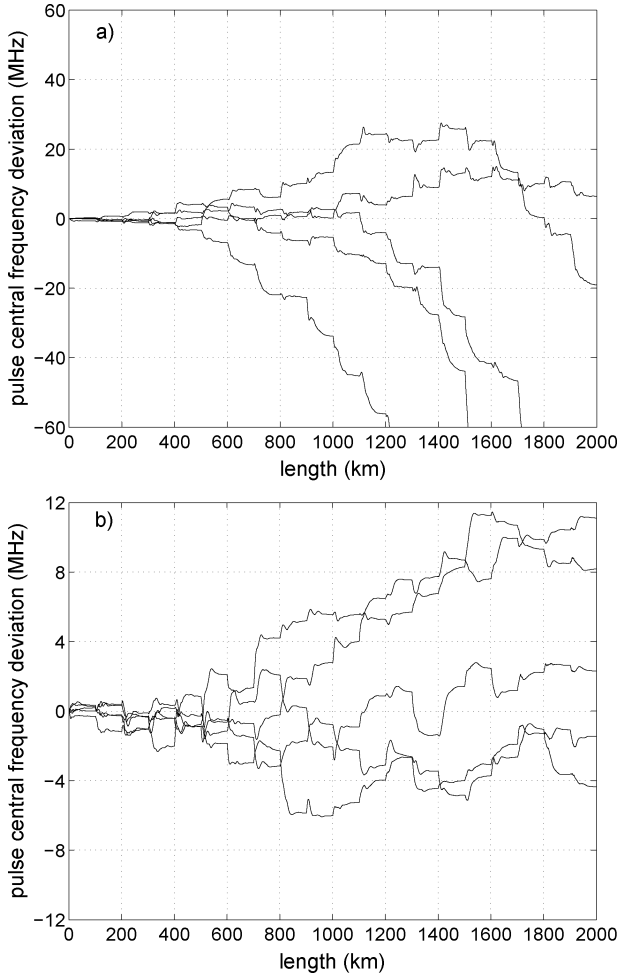

Fig. 2. Pulses' central frequency evolution along a 2000-km-long system. (a) Soliton and (b) nonsoliton communication system are considered. An amplifier is placed every 100 km to compensate for fiber losses. Large frequency shifts tend to occur right after the amplifiers, where the signal and noise powers are highest.

but, as can be seen, it could last several amplification stages. Another feature that can be observed in Fig. 2 is that the absolute value of the frequency shifts tends to increase with the distance; this is a direct consequence of the accumulation of amplified spontaneous emission noise with the propagation distance.

V. Timing Jitter

Experimentally, we do not measure individual symbol's central position or frequency. Usually, we have to rely on a few averaging quantities. Typically, in an experimental setup, it is possible to obtain the first two moments of the electrical pulse position using, for instance, a digital oscilloscope [9], [10]. We can express these two moments, in a given time window, as

$$\overline{t'_t(z)} = \overline{t'_s(z) + t'_n(z) + t'_{sn}(z)} \tag{24}$$

and

$$\overline{t'^2_t(z)} = \overline{[t'_s(z) + t'_n(z) + t'_{sn}(z)]^2} \tag{25}$$

with

$$t'_s(z) = \frac{1}{E_s(z)} \int_{-T_w/2}^{+T_w/2} t\,|S'(z,t)|^2 dt \tag{26}$$

$$t'_n(z) = \frac{1}{E_s(z)} \int_{-T_w/2}^{+T_w/2} t\,|N'(z,t)|^2 dt \tag{27}$$

and

$$t'_{sn}(z) = \frac{1}{E_s(z)} \int_{-T_w/2}^{+T_w/2} t\,S'(z,t)N'^*(z,t)\,dt + \frac{1}{E_s(z)} \int_{-T_w/2}^{+T_w/2} t\,N'(z,t)S'^*(z,t)\,dt \tag{28}$$

where $S'(z,t)$ and $N'(z,t)$ are the filtered signal and noise, respectively, at the photodetector input. We are assuming that a narrow-band optical filter is placed before the photodetector. Typically, the bandwidth of this filter is larger than the signal bandwidth. Therefore this filter does not produce major changes on the signal but removes most of the noise that is outside of the signal bandwidth.

The photocurrent generated by the photodetector due to the incident field is usually further amplified and filtered. The purpose of this electrical processing is to rescale and reshape the signal before the decision circuit in order to minimize the bit error rate of the transmission system. Typically, this electrical processing does not have a major impact on the timing jitter; therefore it is not formally addressed in this paper. Indeed, we run the simulations with and without a matched filter after the photodetector and the results are mostly unaffected as long as a narrow optical filter is placed before the photodetector in order to eliminate most of the out-of-band noise.

Placing a narrow-band optical filter before the photodetector reduces substantially the impact of the noise-to-noise beating. If we also choose a time window T_w on the order of the bit period, the absolute value of $t'_n(z)$ tends to be quite small comparatively with the values of $t'_s(z)$ and $t'_{sn}(z)$.

In order to increase the system reach, we decrease the distance between amplifiers to 40 km. With this new configuration, the peak power required to generate and maintain the fundamental soliton is reduced to 8.3 mW. We consider several systems up to 3800 km. We do not extend the system reach behind 3800 km because modulation instabilities start to appear in the soliton communication system, which would require some sort of in-line control to preserve the solitons. In the soliton communication system, chromatic dispersion is balanced by the Kerr effect. In the nonsoliton system, we use 32 km of standard single-mode fiber followed by 8 km of dispersion compensation fiber per span to balance the chromatic dispersion. The group velocity dispersion assumes the value of -2 and 8 ps^2/km for the standard and dispersion compensation fiber, respectively. Apart from these modifications, the systems configuration is identical to those presented previously.

For all of the considered systems, the absolute value of $t'_{sn}(z)$ tends to be the larger one. Evolution with the distance of $t'_s(z)$, $t'_n(z)$, $t'_{sn}(z)$, and $t'_t(z)$ is presented in Fig. 3 for a particular

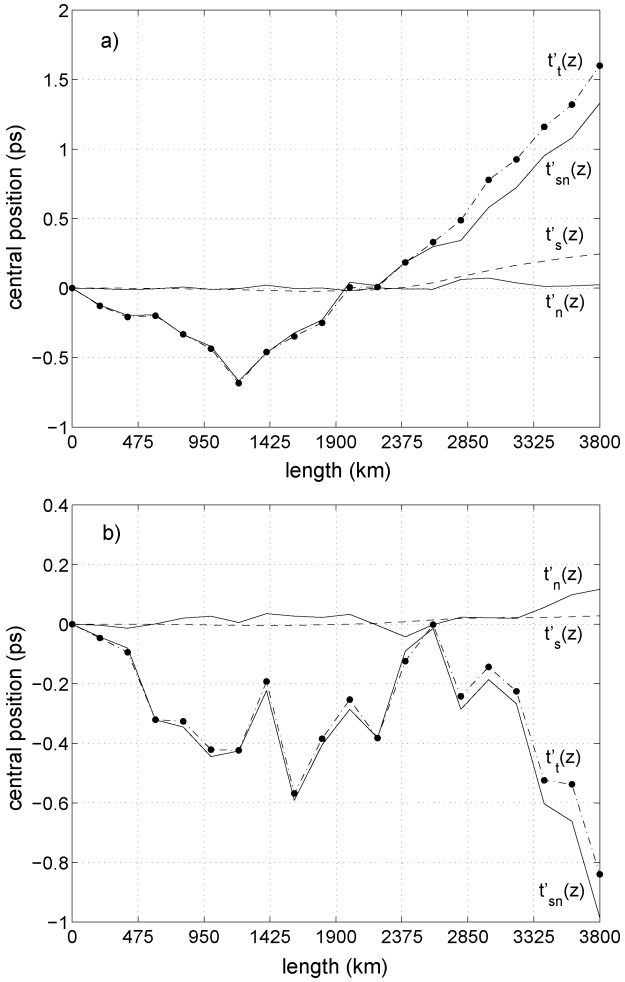

Fig. 3. Temporal deviation due to the signal-to-noise interaction mediated by the Kerr effect ($t'_s(z)$, dashed line), noise-to-noise beating ($t'_n(z)$, full line), and signal-to-noise beating ($t'_{sn}(z)$, full line). The total central position deviation $t'_t(z)$ obtained from the sum of the three contributions is presented as a dash-dot line. The filled circles represent the values obtained using the NLS equation. (a) Soliton and (b) nonsoliton system.

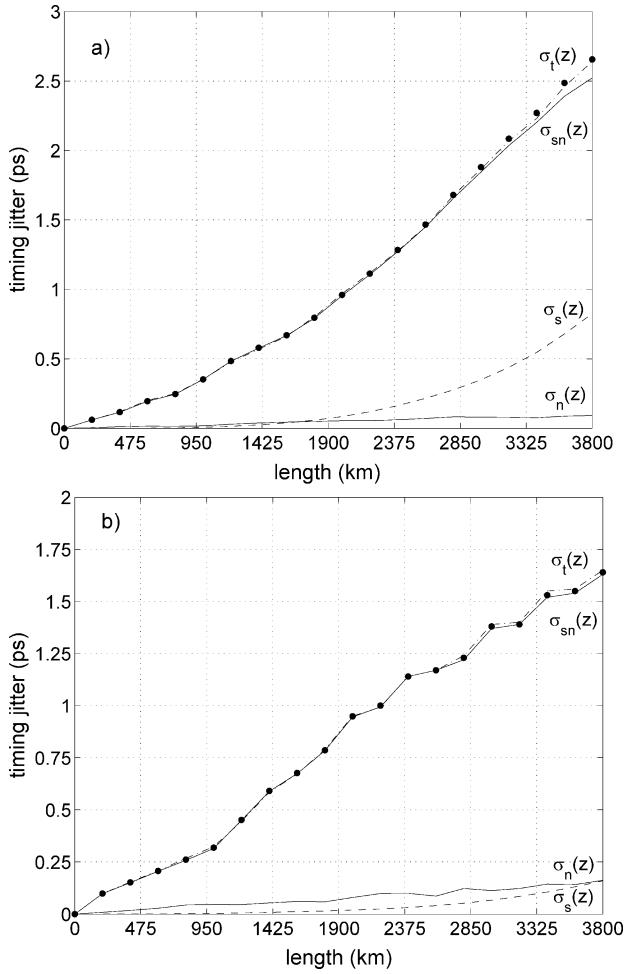

Fig. 4. Timing jitter evolution for (a) soliton and (b) nonsoliton communication system. The total jitter is given by σ_t (dash-dot line), which has three contributions, σ_n (noise-to-noise beating), σ_{sn} (signal-to-noise beating, full line), and σ_s (signal and noise interaction due to the Kerr effect, dashed line). Filled circles represent the values obtained solving the NLS equation.

noise realization, and for (a) soliton and (b) nonsoliton communication systems. Filled circles represent the values obtained by solving the NLS equation directly. It is worth stressing that using the NLS equation we can only estimate the total central position evolution; it is not possible to estimate each contribution separately.

From (24) and (25), we can define the timing jitter as

$$\sigma_t(z) = \sqrt{\overline{t'^2_t(z)} - \overline{t'_t(z)}^2}. \tag{29}$$

Assuming that $t'_s(z)$, $t'_n(z)$, and $t'_{sn}(z)$ are independent random variables, we obtain

$$\sigma^2_t(z) = \sigma^2_s(z) + \sigma^2_n(z) + \sigma^2_{sn}(z) \tag{30}$$

where

$$\sigma^2_s(z) = \overline{t'^2_s(z)} - \overline{t'_s(z)}^2 \tag{31}$$

$$\sigma^2_n(z) = \overline{t'^2_n(z)} - \overline{t'_n(z)}^2 \tag{32}$$

and

$$\sigma^2_{sn}(z) = \overline{t'^2_{sn}(z)} - \overline{t'_{sn}(z)}^2. \tag{33}$$

Using (18) and (19) in conjugation with (26)–(28) and (31)–(33), it is possible to estimate separately the contribution of each component to timing jitter.

In Fig. 4, we present results for the timing jitter for the same systems considered in Fig. 3. From the results in Fig. 4, we can see that the contribution of the noise-to-noise beating for the timing jitter is quite small. Clearly, the major contribution came from the signal-to-noise beating in the photodetector. The contribution due to the signal and noise interaction mediated by the Kerr effect assumes a significative contribution only for large distances. This contribution is in the femtoseconds range for distances up to 1000 km, which is consistent with the results presented in [11]. We can also see that the results obtained solving the NLS equation, circles in Fig. 4, agree well with the results obtained by estimating each contribution for the timing jitter separately and after using (30) to estimate the total timing jitter. This good agreement proves again that (18) and (19) provide a

good model to study the interaction between the signal and noise mediated by the Kerr effect in optical fibers and also shows that the previous assumption that $t'_s(z)$, $t'_n(z)$, and $t'_{sn}(z)$ are independent random variables is acceptable.

VI. Conclusion

We point out that the NLS equation cannot provide information regarding central time position and frequency evolution of symbols that copropagate with noise in optical fibers. This happens because the NLS equation describes the combination of signal and noise as one unit. We show that it is possible to split the NLS equation in two equations: one describing the signal propagation and another describing the noise propagation. Using this pair of equations, one can analyze the symbols' central time position and frequency evolution. We prove that the nonlinear interaction between the signal and noise mediated by the Kerr effect leads to random frequency shifts in all kinds of systems. These random frequency shifts occur during the transmission and are more intense when signal and noise powers are highest, typically right after each amplifier. The absolute value of the central frequency deviation can easily be on the order of some tens of megahertz and therefore must be considered at least in systems using coherent detection. Using our model, it is also possible to estimate the different contributions to timing jitter. We use a realistic model for a direct detection optical receiver in which a narrow-band optical filter is used to remove most of the noise outside the signal spectrum. We found that the dominant contribution to timing jitter tends to be the signal-to-noise beating at the photodetector.

References

[1] L. F. Mollenauer and J. P. Gordon, *Solitons in Optical Fibers: Fundamental and Applications*. New York: Academic, 2006.

[2] J. P. Gordon and H. A. Haus, "Random walk of coherently amplified solitons in optical fiber transmission," *Opt. Lett.*, vol. 11, no. 10, pp. 665–667, 1986.

[3] A. N. Pinto, G. P. Agrawal, and J. F. da Rocha, "Effect of soliton interaction on timing jitter in communication systems," *J. Lightw. Technol.*, vol. 16, no. 4, pp. 515–519, 1998.

[4] T. Georges, "Perturbation theory for the assessment of soliton transmission control," *Opt. Fiber Technol.*, vol. 1, no. 2, pp. 97–116, 1995.

[5] A. N. Pinto, J. F. da Rocha, Q. Lin, and G. P. Agrawal, "Optical versus electrical dispersion compensation: Role of timing jitter," *J. Lightwave Technol.*, vol. 24, pp. 387–395, 2006.

[6] A. N. Pinto and G. P. Agrawal, "Noise-induced spectral shifts in pseudo-linear fiber-optic communication systems," in *Proc. Conf. Lasers Electro-Opt.*, Baltimore, MD, 2007.

[7] G. P. Agrawal, *Lightwave Technology: Telecommunication Systems*. Hoboken, NJ: Wiley, 2005.

[8] H. Toda, K. Hamada, Y. Furukawa, Y. Kodama, and S. Seikai, "Experimental evaluation of Gorsdon-Haus timing jitter of dispersion managed solitons," in *Proc. 25th Eur. Conf. Opt. Commun.*, Nice, France, 1999, vol. I, pp. 406–407.

[9] R. Holzlöhner, H. N. Ereifej, V. S. Grigoryan, G. M. Carter, and C. R. Menyuk, "Experimental and theoretical characterization of a 40-Gb/s long-haul single-channel transmission system," *J. Lightw. Technol.*, vol. 20, no. 7, pp. 1124–1131, 2002.

[10] H. Xu, J. Zweck, L. Yan, C. R. Menyuk, and G. M. Carter, "Quantitative experimental study of intrachannel nonlinear timing jitter in a 10-Gb/s terrestrial WDM return-to-zero system," *IEEE Photon. Technol. Lett.*, vol. 16, pp. 314–316, 2004.

[11] M. Westlund, H. Sunnerud, J. Li, J. Hansryd, M. Karlsson, and P. A. Andrekson, "Measurement of ultralow Gordon-Haus timing jitter in dispersion-managed soliton systems," *IEEE Photon. Technol. Lett.*, vol. 14, pp. 1097–1099, 2002.

Armando N. Pinto (M'00–SM'06) received the bachelor's degree in electronic and telecommunications engineering and the Ph.D. degree in electrical engineering from the University of Aveiro, Aveiro, Portugal, in 1994 and 1999, respectively.

In 2000, he became an Assistant Professor in the Electrical, Telecommunications and Informatics Department, University of Aveiro, and a Researcher with the Institute of Telecommunications, Aveiro. During academic year of 2006–2007 he was a Visiting Professor at the Institute of Optics, University of Rochester, Rochester, NY. His main research interests focus on optical communication systems, mainly in nonlinear, polarization, and quantum effects in fiber optics. He has published more than 80 scientific papers in international journals and conferences.

Dr. Pinto is a member of the Optical Society of America.

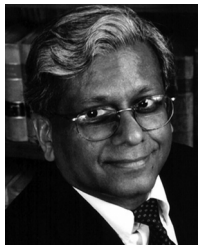

Govind P. Agrawal (M'83–SM'86–F'96) received the B.S. degree from the University of Lucknow, India, in 1969 and the M.S. and Ph.D. degrees from the Indian Institute of Technology, New Delhi, in 1971 and 1974, respectively.

After positions with the Ecole Polytechnique, France, the City University of New York, New York, and AT&T Bell Laboratories, Murray Hill, NJ, in 1989 he joined the Faculty of the Institute of Optics, University of Rochester, Rochester, NY, where he is a Professor of optics. His research interests focus on optical communications, nonlinear optics, and laser physics. He is an author or coauthor of more than 300 research papers, several book chapters and review articles, and seven books, most recently *Nonlinear Fiber Optics* (Boston, MA: Academic Press, 4th ed., 2007). He has participated in organizing multiple technical conferences. He was General Cochair for the Quantum Electronics and Laser Science Conference in 2001 and a member of the Program Committee for the Conference on Lasers and Electro-Optics in 2004 and 2005.

Dr. Agrawal is a Life Fellow of the Optical Society of India and a Fellow of the Optical Society of America.